The Astrophysical Journal, 841:77 (10pp), 2017 June 1 https://doi.org/10.3847/1538-4357/aa6f5e

Binary Black Hole Mergers from Field Triples: Properties, Rates, and the Impact of Stellar Evolution

Fabio Antonini[1,4], Silvia Toonen[2,4], and Adrian S. Hamers[3]
[1] Center for Interdisciplinary Exploration and Research in Astrophysics (CIERA) and Department of Physics and Astrophysics, Northwestern University, Evanston, IL 60208, USA
[2] Astronomical Institute Anton Pannekoek, University of Amsterdam, P.O. Box 94249, 1090 GE, Amsterdam, The Netherlands
[3] Institute for Advanced Study, School of Natural Sciences, Einstein Drive, Princeton, NJ 08540, USA
Received 2017 March 20; revised 2017 April 19; accepted 2017 April 19; published 2017 May 25

Abstract

We consider the formation of binary black hole (BH) mergers through the evolution of field massive triple stars. In this scenario, favorable conditions for the inspiral of a BH binary are initiated by its gravitational interaction with a distant companion, rather than by a common-envelope phase invoked in standard binary evolution models. We use a code that follows self-consistently the evolution of massive triple stars, combining the secular triple dynamics (Lidov–Kozai cycles) with stellar evolution. After a BH triple is formed, its dynamical evolution is computed using either the orbit-averaged equations of motion, or a high-precision direct integrator for triples with weaker hierarchies for which the secular perturbation theory breaks down. Most BH mergers in our models are produced in the latter non-secular dynamical regime. We derive the properties of the merging binaries and compute a BH merger rate in the range (0.3–1.3) $\mathrm{Gpc^{-3}\,yr^{-1}}$, or up to $\approx$2.5 $\mathrm{Gpc^{-3}\,yr^{-1}}$ if the BH orbital planes have initially random orientation. Finally, we show that BH mergers from the triple channel have significantly higher eccentricities than those formed through the evolution of massive binaries or in dense star clusters. Measured eccentricities could therefore be used to uniquely identify binary mergers formed through the evolution of triple stars. While our results suggest up to $\approx$10 detections per year with Advanced-LIGO, the high eccentricities could render the merging binaries harder to detect with planned space based interferometers such as LISA.

Key words: stars: black holes – stars: massive

1. Introduction

The recent breakthrough detection of gravitational waves (GWs) from merging black hole (BH) binaries by Advanced-LIGO (aLIGO) has generated enormous interest in understanding how these sources form (Abbott et al. 2016a, 2016b, 2016c). With the many hundreds to thousands of merging binary signals now expected to be detected in upcoming years, the numerical and analytical modeling of the formation of compact-object binaries will be central for a correct astrophysical interpretation of the GW sources we are about to discover (Abbott et al. 2016d).

Several channels for the formation of BH binary mergers have been proposed. Binary BHs can form as the result of (1) the evolution of isolated massive binaries in galactic fields (Belczynski et al. 2010, 2016; Mandel & de Mink 2016); (2) dynamical interactions in galactic nuclei, with and without a massive BH (Antonini & Perets 2012; Antonini & Rasio 2016); (3) dynamical exchange interactions in the dense stellar core of globular clusters (Rodriguez et al. 2015; Haster et al. 2016; Chatterjee et al. 2017) or young massive star clusters (Banerjee 2017); (4) the evolution of isolated triples in galactic fields (Silsbee & Tremaine 2017), leading to a merger of the inner binary through the Lidov–Kozai mechanism (LK; Kozai 1962; Lidov 1962) coupled with energy loss due to GW radiation (e.g., Thompson 2011; Antonini et al. 2014; Kimpson et al. 2016).

In this paper, we make precise predictions for scenario (4). We use a numerical algorithm (Toonen et al. 2016) that combines the secular triple dynamics with stellar evolution and interactions to follow the evolution of stellar triples and the way this results in the formation of BH triples. After their formation, the BH triples are evolved forward in time using either the octupole level secular equations of motion of triple systems (e.g., Blaes et al. 2002; Naoz et al. 2013) or a high-precision direct integrator for systems with weaker hierarchies where the secular equations become inaccurate (Mikkola & Merritt 2008). Unlike previous studies (e.g., Silsbee & Tremaine 2017) our models follow the stellar, binary, and triple evolution self-consistently together with the triple secular dynamics, prior to the formation of the triple BH system. We perform a population synthesis study that allows us to make concrete predictions about the merger rate and properties of BH binaries formed in massive field triples.

The paper is organized as follows. In Section 2, we describe the numerical method and, in Section 3, we describe our choice for the initial conditions. In Section 4, we present the main results of our simulations and compute the properties and merger rate of binary BHs formed in our models. In Section 5, we discuss the importance of the non-secular dynamical regime and possible effects related to encounters with field stars. Section 6 provides a summary.

2. Method

To simulate the formation of triple BH systems, we use the recently published code `TRES` (Toonen et al. 2016) for studying the evolution of coeval, dynamically stable, hierarchical, stellar triples. The simulations start with three stars on the zero-age main sequence in a specific orbital configuration. Consequently, the evolution of the stars and the orbit is followed in time. Stellar evolution is modeled in a parametrized way through the fast stellar evolution code SeBa (Toonen et al. 2012).

[4] Contributed equally to this work.

The parametrization is originally based on analytic formulae that are fitted to detailed stellar evolution calculations of single stars (Hurley et al. 2000). Mass loss from stellar winds is incorporated as in Toonen & Nelemans (2013). The wind mass-loss rates are time-dependent and reflect the stellar phase and parameters (e.g., luminosity and radius).

The secular orbital evolution of the triple is modeled by solving a set of ordinary differential equations (ODEs) for the inner and outer orbital elements and the spin frequencies of the bodies, similarly to Hamers et al. (2013). In addition to the secular three-body dynamics, we include tidal evolution (dissipation and precession due to tidal bulges) in the inner binary, assuming the equilibrium tide model and stellar spins parallel to the orbit (Hut 1981), general relativistic corrections (precession at the 1PN order and GW emission at the 2.5PN order), and orbital changes associated with stellar winds. During the ODE integration, we check for dynamical instability using the Mardling & Aarseth (2001) stability criterion, and for the onset of mass transfer using the results of Sepinsky et al. (2007; see also Dosopoulou & Kalogera 2016a, 2016b). The latter can be triggered by eccentricity driving by LK oscillations, though the subsequent evolution is not taken into account here; instead, we track the onset of mass transfer in our simulations and do not model the further evolution.

Antonini et al. (2014) show that the angular momentum of the inner binary can change by order of itself in one orbital period if

$$\sqrt{1-e_1} \lesssim \sqrt{1-e_{\rm crit}} \equiv 5\pi \frac{m_3}{m_1+m_2}\left[\frac{a_1}{a_2(1-e_2)}\right]^3, \quad (1)$$

where e_1 (e_2) and a_1 (a_2) are the eccentricity and semimajor axis of the inner (outer) binary, and m_1+m_2 and m_3 are the total mass of the inner binary and the mass of the tertiary companion, respectively. In what follows, we refer to the high-e region of parameter space defined by Equation (1) as the "non-secular" dynamical regime. If the eccentricity of the inner binary becomes larger than $e_{\rm crit}$, the outer perturber can significantly change the angular momentum of the eccentric binary at the last apoapsis passage leading to a jump in angular momentum of the order of unity (see Antonini & Perets, and Equation (7) in Katz & Dong 2012). In this situation, the secular equations of motion (e.g., Naoz 2016) become a poor approximation. For this reason, during the secular integrations, we checked whether e_1 became larger than $e_{\rm crit}$. If this happened, we reintegrated the evolution of the BH triple system using the direct code AR-CHAIN (Mikkola & Merritt 2008). The AR-CHAIN code combines the use of the chain regularization method and the time-transformed leapfrog scheme to avoid singularities, and includes relativistic effects to the motion that are added as 1, 2, and 2.5 order post-Newtonian corrections. We assumed that the orbital phases were initially random and ran our direct integrations up to a maximum time of 10 Gyr. For most triples, this maximum time corresponds to a few thousand times the LK timescale (Holman et al. 1997):

$$T_{\rm LK} = P_1 \left(\frac{m_1+m_2}{m_3}\right)\left(\frac{a_2}{a_1}\right)^3 (1-e_2^2)^{3/2}, \quad (2)$$

with P_1 the orbital period of the inner binary.

3. Initial Conditions

3.1. Orbit and Mass Distributions

The stellar triples in our simulations are initialized as described in what follows. In total, we consider six different models (see Table 1).

In all of our models, we assume solar metallicity and sample the mass of the most massive star in the inner binary from a Kroupa initial mass function (Kroupa 2002). We adopt a flat mass ratio distribution between 0 and 1 for both the inner binary, i.e., m_2/m_1, and the outer binary, i.e., $m_3/(m_1+m_2)$. This choice is consistent with observations of massive binary stars, which indicates a nearly flat distribution of the mass ratio (e.g., Sana et al. 2012; Duchêne & Kraus 2013; Kobulnicky et al. 2014). Stellar masses were sampled in the range [22 $M_\odot$, 100 $M_\odot$] for m_1 and m_2, and in the range [$m_{3,\rm min}$, 100 $M_\odot$] for the outer star. In models A1, B1, and C1, we set $m_{3,\rm min} = 0.1$ $M_\odot$; in models A2, B2, and C2, we set $m_{3,\rm min} = 22$ $M_\odot$. The upper limit on the mass comes from the fact that the stellar evolution tracks used in TRES are not valid above 100 $M_\odot$.

The distribution of orbital separations/periods is often assumed to be flat in log-space (Öpik's law). However, Sana et al. (2012) find that the orbital periods follow a power-law function $\log(P/{\rm days})^{-0.55}$, in the range (0.15–5.5); while, for wide orbits, there are indications that the distribution is more similar to the canonical Öpik's law. Hence, we take $N \propto \log(P_1/{\rm days})^{-0.55}$ for the period of the inner binary, and flat in log-space for the period of the outer orbit.

Any common-envelope phase of evolution will likely shrink the inner orbit so that the Lidov–Kozai mechanism will become more strongly suppressed by the relativistic precession of the inner binary orbit (e.g., Blaes et al. 2002). For this reason, in order to make sure that the periapsis distance of the inner binary is large enough that no common-envelope phase or mass transfer occurs, we impose a minimum orbital separation $a_1(1-e_1^2) \geqslant 2500\,R_\odot \approx 11$ au. The latter is the maximum radius of a low-mass BH progenitor (e.g., Toonen & Nelemans 2013). We have placed a conservative limit by using the semi-latus rectum instead of the periapsis of the orbit, because in this way we exclude binaries that would experience mass transfer even if they would be isolated, as tides would circularize the binary to the semi-latus rectum. We also imposed a maximum separation, $a_{2,\rm max}$, for the outer star. In models A1, B1, and C1, we set $a_{2,\rm max} = 5\times10^6\ R_\odot = 2.2\times10^4$ au; in models A2, B2, and C2, we set $a_{2,\rm max} = 5\times10^5\ R_\odot = 2.2\times10^3$ au.

For the orbital eccentricities of the inner binary, e_1, and outer binary, e_2, we adopt a flat distribution between 0 and 1.

Lastly, we sample the initial orbital inclination angle between the inner and outer orbit, I, randomly in $\cos I$ with $-1 < \cos I < 1$, and the initial arguments of periapsis of inner and outer orbits g_1 and g_2 randomly between 0 and 2π. From the triple systems obtained, we subsequently reject those that are dynamically unstable based on the stability criterion of Mardling & Aarseth (2001).

3.2. Kick Distributions

Any asymmetry in the supernova, such as in the mass or neutrino loss can give rise to a natal-kick to the newly formed compact-object. If the collapsing star is part of a binary or triple, the natal kick alters the orbit. If the overall kinetic energy imparted through the natal kicks is higher than the binding

Table 1
Results of the Population Synthesis Models of Massive Triple Stars

Model	Natal Kicks	$a_{2;\max}$ (10^3 au)	$m_{3;\min}$ ($M_\odot$)	$N_{\rm sim}$	Fraction Disrupted	Fraction Mass Transfer	Fraction Dyn. Unstable	$\epsilon_{\rm 3BH}$	$\epsilon_{\rm merge}$	Γ (Gpc^{-3} yr^{-1})
A1	0	20	0.1	50k	0.31	0.27	0.19	0.18	6×10^{-3}	1.3
A2	0	2	22	50k	0.14	0.43	0.22	0.21	7×10^{-3}	1.2
B1	Hobbs	20	0.1	25k	0.56	0.26	0.12	0.06	5×10^{-3}	0.4
B2	Hobbs	2	22	25k	0.36	0.41	0.17	0.06	1×10^{-2}	0.5
C1	Arzoumanian	20	0.1	25k	0.56	0.26	0.13	0.05	8×10^{-3}	0.5
C2	Arzoumanian	2	22	25k	0.35	0.42	0.17	0.06	5×10^{-3}	0.3

Note. Models differ by their natal kick velocity distribution, adopted maximum value of separation, $a_{2,\max}$, and minimum mass, $m_{3;\min}$, of the tertiary star. $N_{\rm sim}$ is the total number of stellar triples that were evolved for each model; $\epsilon_{\rm 3BH}$ is the fraction of systems that produce stable BH triples; $\epsilon_{\rm merge}$ is the fraction of the stable BH triples that lead to the merger of a BH binary; and Γ is the inferred BH binary merger rate.

energy of the binary orbit, the supernova kick can fully unbind the system. We assume that the supernova is instantaneous and that the supernova-shell does not impact the companion star(s).

In our simulations, the orbital evolution of a triple due to an instantaneous supernova kick was modeled using the procedure described in the appendix of Toonen et al. (2016). In summary, the positions and velocities of the three bodies before and just after the supernova are computed from the orbital elements assuming a random mean anomaly and assuming no changes in the position vectors. To the body undergoing the supernova, the natal kick velocity is added to the orbital velocity and the mass is updated. Consequently, we compute the new eccentricity and specific angular momentum vectors for the inner and outer orbits, and the new orbital elements are computed from these vectors. Note that the total orbital angular momentum vector of the triple is not conserved because of the mass loss and the natal kick velocity. Therefore, the reference plane for the orbital elements (i.e., the invariable plane perpendicular to the total orbital angular momentum vector) changes due to the supernova, and our approach takes this effect into account.

The distribution of natal kick velocities of BHs is unknown. We therefore consider a number of choices for the natal kick velocity (see Table 1). In models A1 and A2, we assume no natal kick during BH formation. We note that even in this case, the binary receives a kick to its center of mass because one of the massive components suddenly loses mass (Blaauw 1961).

In models B1, B2, C1, and C2, we consider a non-zero-kick velocity for the newly formed BHs. We implement momentum-conserving kicks, in which we assume that the momentum imparted on a BH is the same as the momentum given to a neutron star. Thus, the kick velocities for the BHs will be reduced with respect to those of neutron stars by a factor of $m_{\rm NS}/m_{\rm BH}$, with $m_{\rm NS} = 1.4\,M_\odot$ the typical neutron star mass, and $m_{\rm BH}$ the mass of the forming BH. The neutron star kick distributions we adopt are constrained by observations. In models B1 and B2, we use the neutron star kick distribution of Hobbs et al. (2005), which can be approximated by a Maxwellian distribution with dispersion $265\,{\rm km\,s^{-1}}$ for neutron stars, and $\approx 40\,{\rm km\,s^{-1}}$ for BHs after the kick velocities have been reduced by the ratio of BH to neutron star mass. In models C1 and C2, we use the neutron star kick distribution of Arzoumanian et al. (2002). This latter distribution is bimodal with a peak at $\approx 100\,{\rm km\,s^{-1}}$ and a lower peak at $\approx 700\,{\rm km\,s^{-1}}$ for neutron stars; this converts into a kick distribution for BHs with a main peak at $\approx 20\,{\rm km\,s^{-1}}$ and a lower peak at $\approx 120\,{\rm km\,s^{-1}}$.

Finally, in all of our models, we assume that stars with a zero-age main-sequence mass $m \geqslant 40\,M_\odot$ do not receive any natal kick. This is consistent with the direct collapse scenario described in Fryer & Kalogera (2001), where the fallback completely damps any natal kick for $m \gtrsim 40\,M_\odot$, assuming solar metallicity.

4. Results

In this section, we describe the key physical properties and merger rates of the BH binaries/triples in our models. In total, we observe 177 BH mergers among the 200,000 systems we evolved. We note that systems other than BH triples also produce mergers in our simulations. Main-sequence stars that do not evolve to a compact object within one Hubble time are unlikely to result in efficient LK cycles due to their lower mass. Accordingly, we did not find any mergers for systems in which the tertiary was still on the main sequence at the end of the simulation. In our models with low-mass tertiaries (i.e., models A1, B1, and C1), we found that 8 out of a total of 75 mergers were produced in triples in which the tertiary was not a BH. In three of these systems, the tertiary companion became a neutron star by the end of the simulation, in three others the tertiary became a CO white dwarf, and in the remaining two the tertiary became an ONe white dwarf.

Figure 1 shows the results of a three-body direct integration of one BH triple system that leads to the formation of a BH merger. The secular exchanges of angular momentum (but not energy) among the inner binary and the outer BH induce large fluctuations in the inner binary eccentricity and inclination. The orbit of the inner binary, starting from an initial value of $e_1 = 0.65$ and $I = 93.^\circ 8$, diffuses to $1 - e_1 \approx 1 \times 10^{-4}$ by $\approx 3 \times 10^6$ year. We find that the maximum orbital eccentricity of the inner binary undergoes a random walk to most of the phase space allowed by the total energy and angular momentum of the system. During the maximum of an LK oscillation, the binary enters the non-secular regime defined by Equation (1). In this region, the inner BHs can be driven to a merger before general relativistic effects suppress the secular forcing. At the end of the integration, GW radiation starts to dominate the binary evolution. Subsequently, the BH binary starts to circularize, decouples from the tertiary companion, and finally enters the 10 Hz aLIGO frequency band with $e_1 = 0.4$ and $a_1 = 1.5 \times 10^{-5}$ au.

4.1. Properties

Table 1 gives the fraction of systems that undergo mass-transfer, that are disrupted due to supernova kicks, and the

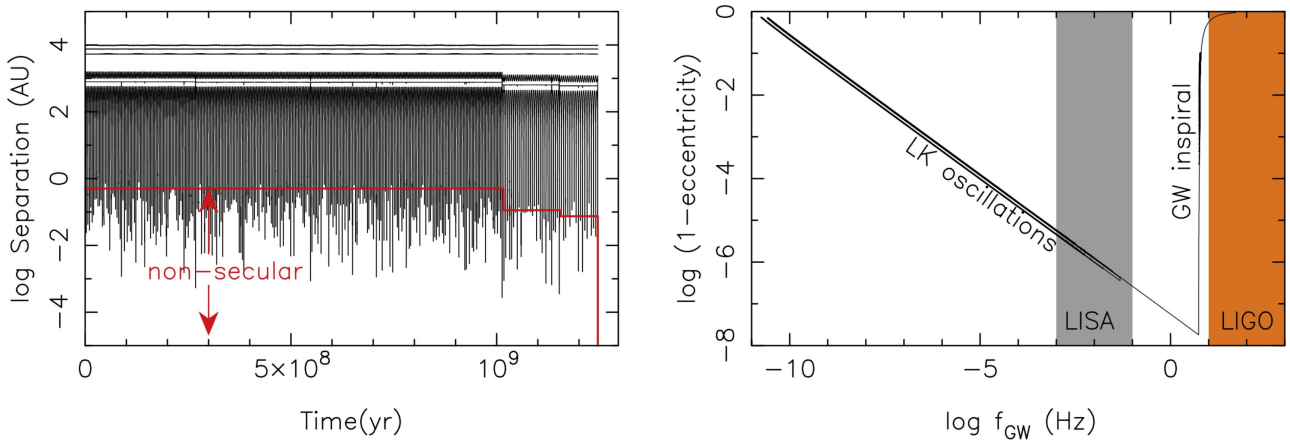

Figure 1. Formation of a BH merger in one of our simulations (AR-CHAIN integration). Masses and initial orbital parameters were as follows: $m_1 = 8.96\ M_\odot$, $m_2 = 7.51\ M_\odot$, $m_3 = 8.35\ M_\odot$, $a_1 = 1727$ au, $a_2 = 16571$ au, $e_1 = 0.65$, $e_2 = 0.29$, $I = 93.^\circ8$, $g_1(\mathrm{rad}) = 0.61$, $g_2(\mathrm{rad}) = -2.82$, and the longitude of the ascending node $\Omega_1(\mathrm{rad}) = -2.4$. Radial excursions of the three BHs (semimajor axis, periapse, and apoapse) are shown as functions of time, with the red line demarcating the region below which the standard secular perturbation theory breaks down according to Equation (1). At $\approx 10^9$ years, the two BHs approach each other closely and energy dissipation due to GW radiation leads to a sudden decrease in the inner binary semimajor axis; at the end of the simulation, after $\approx 1.3 \times 10^9$ years, the inner binary merges. The right panel displays the evolution of the inner binary eccentricity as a function of the peak gravitational wave frequency as defined in Equation (4). The binary evolves into the LISA frequency band, $f_{\rm GW} \gtrsim 10^{-3}$ Hz (Amaro-Seoane et al. 2017), with extremely high eccentricities. The GW driven inspiral starts at $f_{\rm GW} \approx 5$ Hz, outside the LISA frequency window. By the time the binary reaches the 10 Hz frequency, its eccentricity is $e_1 \approx 0.4$.

fraction of stable BH triples, $\epsilon_{\rm 3BH}$, that are formed in our models. The rest of the systems became dynamically unstable (Mardling & Aarseth 2001) during their evolution due to, e.g., stellar wind mass loss (Perets & Kratter 2012) and supernova kicks. Simulations with the smaller range of masses/orbits (models A2, B2, and C2) show fewer systems that are disrupted due to the supernova kicks, more systems that experience mass transfer, and an almost unchanged fraction of stable BH triples. Compared to models with no kicks, the simulations with non-zero birth kicks (models B1, B2 and C1, C2) show more systems that are disrupted due to the supernova kicks, and, consequently, fewer stable BH triples formed.

In Figure 2, we show the distribution of the inclination between inner and outer orbit of the initial BH triples (black histograms), and of the subset of these that produce BH mergers (red histograms). Figure 2 shows that essentially all merging binaries are formed in triples with high inclination and in the range $70^\circ \lesssim I \lesssim 110^\circ$. The initial BH triples are formed with a distribution, which is clearly anisotropic, with a deficit of orbits near $\cos I = 0$. This is a consequence of many initially highly inclined systems that, due to the LK mechanism, merge or undergo a phase of mass transfer before the three BHs are formed. This effect, similarly occurring in the evolution of lower-mass triples (Hamers et al. 2013), reduces the number of BH triple systems with high inclination, which can lead to a BH binary merger, lowering the overall BH merger rate compared to what we would obtain by assuming an initially random distribution of inclinations (e.g., Silsbee & Tremaine 2017).

Figure 2 shows that the I distribution of BH triples with initially larger semimajor axes is closer to isotropic. The reason for this is that systems where the tertiary is at a larger separation are less likely to merge during their main-sequence evolution given their longer LK timescales (see Equation (2)) and that the e-oscillations are more strongly quenched by precession of the periapsis due to relativity or due to tidal bulges for larger values of a_2/a_1 (e.g., Blaes et al. 2002; Fabrycky & Tremaine 2007).

Figure 3 gives the distribution of the semimajor axes a_1 and a_2 at the moment the triple BHs are formed and for the subset of the BH triples that lead to merging binaries. These plots show that our mergers are produced in BH triples with $a_1 \gtrsim 100$ au and $a_2 \gtrsim 1000$ au. The left panels of Figure 3 give the distribution of the ratio $a_2(1-e_2)/a_1$. This latter quantity parametrizes how well the dynamics of the system can be described by the standard secular equations of motion. The non-secular region in Figure 3 was computed from Equation (1) by requiring the inner BH binary to reach an eccentricity large enough for GW radiation to dominate its evolution. One finds that the inner binary can enter the non-secular regime if (Antonini et al. 2016)

$$\frac{a_2(1-e_2)}{a_1} \lesssim 2.5\left(\frac{m_3}{m_1+m_2}\right)^{1/3}\left(\frac{a}{D_{\rm diss}}\right)^{1/6}, \qquad (3)$$

with $D_{\rm diss}$ the typical dissipation scale. Most of our binaries are driven to a merger from an initial distance $a_1 \gtrsim 100$ au. Adopting $D_{\rm diss} = 10^9$ cm as a conservative dissipation scale and assuming equal-mass components, we find that the condition Equation (1) is met before GW radiation dominates the evolution of the inner binary if $a_2(1-e_2)/a_1 \lesssim 20$. We stress that not all triples that are within the blue vertical lines in Figure 3 enter the non-secular regime, but only those that achieve an eccentricity $e_1 \gtrsim e_{\rm crit}$. The red histograms in Figure 3 represent the binaries that merge in our models. Evidently, most merging binaries in our simulations are expected to evolve through the non-secular dynamical regime defined by Equation (1); this happened for 132 of the 177 total mergers we found.

The left panel of Figure 4 displays the distribution of eccentricities at the moment the peak GW frequency of the binaries becomes larger than the 10 Hz aLIGO frequency band. Eccentric binaries emit a GW signal with a broad spectrum of frequencies; we compute a proxy for the GW frequency of our merging binaries as the frequency corresponding to the harmonic, which leads to the maximal emission of GW

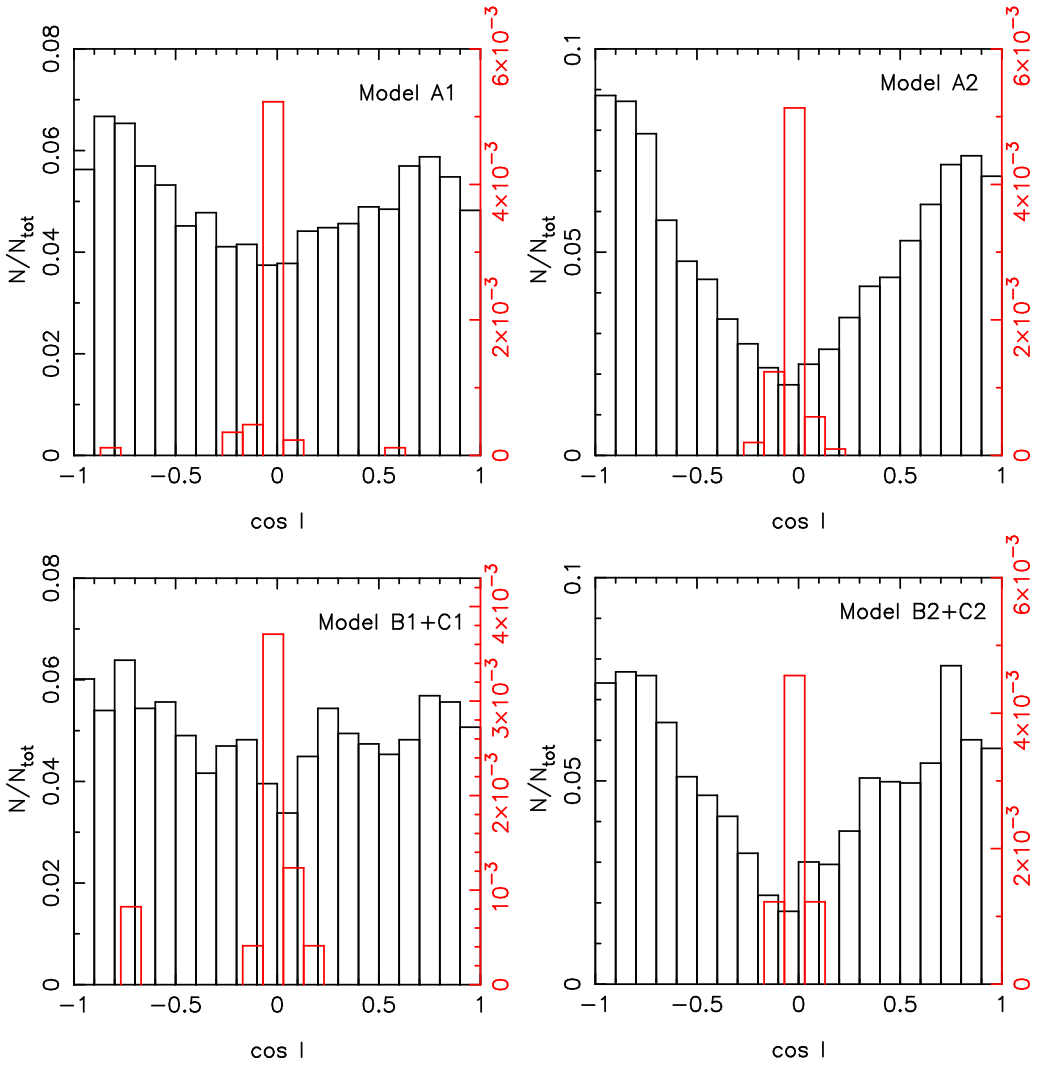

Figure 2. Distribution of relative inclination of outer to inner orbit for the BH triples formed in our models according to the secular population synthesis code (black histograms), and for the triples, which produce BH mergers (red histograms). The number of systems are normalized by the total number of stable BH triples formed. This plot shows that the initial distribution of I is not isotropic and that most merging BH binaries are produced in BH triples with initially high mutual inclinations.

radiation (Wen 2003):

$$f_{\rm GW} = \frac{\sqrt{G(m_1+m_2)}}{\pi}\frac{(1+e_1)^{1.195}}{[a_1(1-e_1^2)]^{1.5}}. \quad (4)$$

About 3% of all merging BH binaries in our models enter the 10 Hz window with an extremely high eccentricity $(1-e_1) \lesssim 10^{-6}$, while ≈90% of them have eccentricities $\lesssim$0.1 at 10 Hz.

In Figure 5, we compare the eccentricity distribution at $f_{\rm GW} = 10$ Hz of our merging BH binaries to those formed in star clusters and from field binaries. These two latter distributions were taken from Figure 3 of Breivik et al. (2016). While the field and cluster models predict similar eccentricity distributions (e.g., Nishizawa et al. 2017), the eccentricities of merging BH binaries from field triples appear to be uniquely biased toward high values. We conclude that eccentricity measurements alone could be potentially used to discriminate binaries formed through the evolution of isolated massive triple stars. However, the high eccentricities found in our models also imply that a fraction of these binaries could emit their maximum power at frequencies much higher than the frequency window of the planned Laser Interferometer Space Antenna (LISA; $f_{\rm GW} \approx [10^{-3}, 0.1]$ Hz). As argued in Chen & Amaro-Seoane (2017), binaries that enter the aLIGO band with $e_1 \gtrsim 5 \times 10^{-3}$ could be harder to detect with instruments like LISA. Of the 177 merging binaries in our simulations, 69 (137) have eccentricities higher than 5×10^{-3} (10^{-3}) and could therefore be harder to detect at lower frequencies.

In the middle panel of Figure 4, we show the distribution of the total and chirp mass of the merging binaries, where this latter is defined as $M_{\rm chirp} = (m_1 m_2)^{3/5}/(m_1+m_2)^{1/5}$. Our merging binaries have total masses in the range [13 $M_\odot$, 20 $M_\odot$] and a chirp mass distribution that peaks around ≈7 $M_\odot$. The merging binaries in models with a non-zero natal kick appear to have larger masses when compared to the models without birth kicks. It is expected that, given our assumption of momentum-conserving kicks, higher mass BHs receive, on average, lower velocity kicks and are therefore more likely to be retained in triples and merge.

The right panel of Figure 4 shows the time delay distribution, where $T_{\rm delay}$ is the time from formation of the BH triple to the merger of the inner BH binary. In models with no birth kicks, about ≈50% of all merging binaries have delay times $\lesssim$1 Gyr,

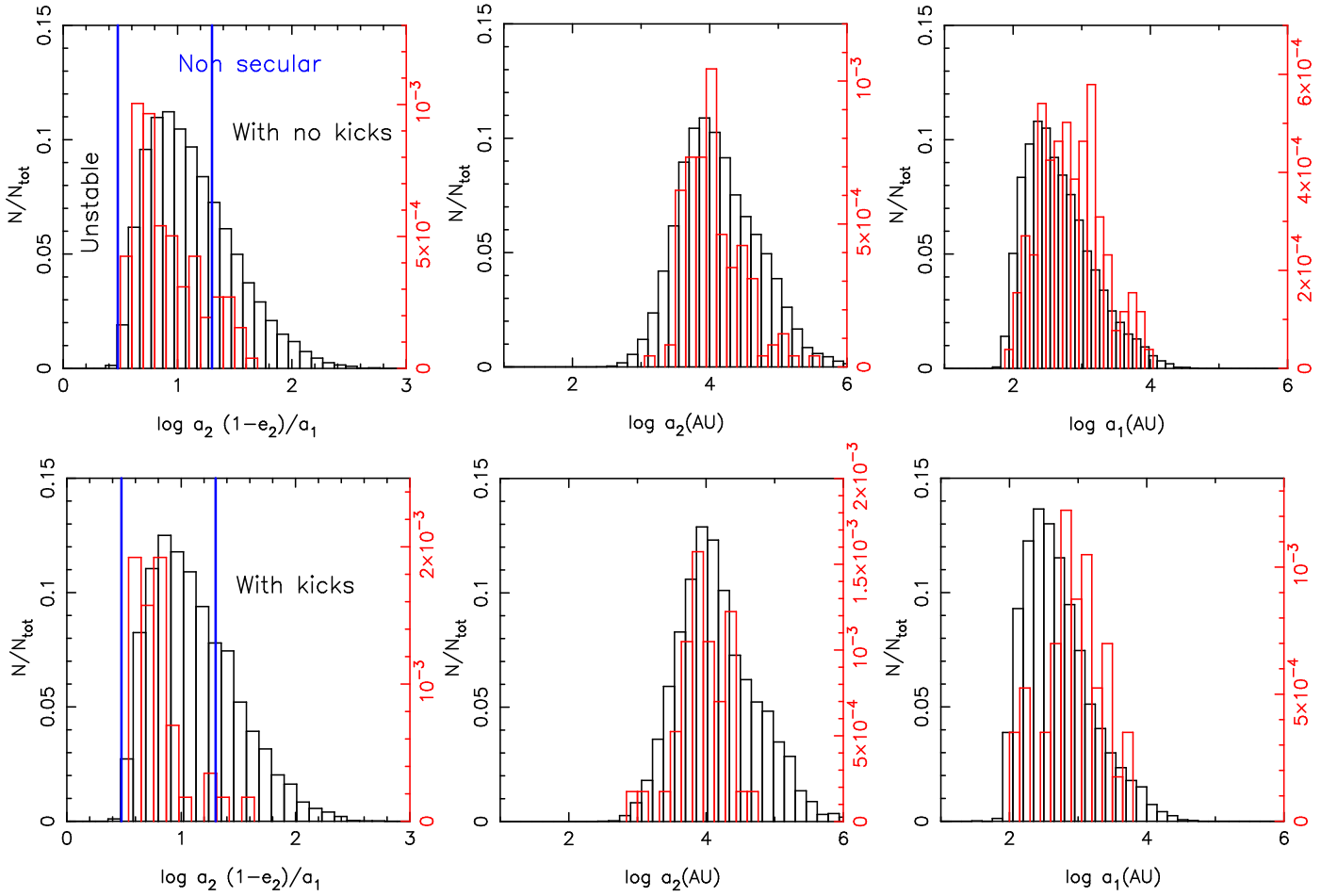

Figure 3. Distribution of orbital separations of the stable BH triples formed in the secular population synthesis simulations (black) and those that lead to a merging BH binary (red). Left panels give the distribution of the minimum distance of the outer BH to the inner binary, divided by the inner BH binary semimajor axes; the middle panels show the distribution of the outer orbit semimajor axes; and the right panels show the distribution of the inner binary semimajor axis. These distributions have been normalized to the total number of BH triples formed. In the left panels, the BH triples that are within the blue vertical lines and achieve an eccentricity $e_1 \gtrsim e_{\rm crit}$ enter the non-secular dynamical regime defined by Equation (1) before GW radiation becomes important to their evolution. Most triples that produce BH mergers are expected to evolve in the non-secular regime where the standard octupole secular equations of motion (e.g., Naoz et al. 2013; Naoz 2016) are not valid. The right panels show that BH binaries formed through the triple channel are driven to a merger from distances $10^2 \lesssim a_1 \lesssim 10^3$ au and have companions at $10^3 \lesssim a_2 \lesssim 10^4$ au.

while this percentage increases to ≈60% in models with non-zero natal kicks. Essentially, all merging binaries have delay times larger than $\approx 10^6$ years. Note that, for a 22 $M_\odot$ star, the time from formation of the star to the formation of the BH is $\lesssim$8 Myr.

4.2. Merger Rates

In order to compute the merger rate of binary BHs, we follow the procedure described in Silsbee & Tremaine (2017). The number of stars formed per unit mass is given by

$$N_\star(m)dm = 5.4 \times 10^6\, m^{-2.3}\ {\rm Gpc}^{-3}\ {\rm yr}^{-1}. \quad (5)$$

Adopting a constant star-formation rate per comoving volume unit, the merger rate of binary BHs is then

$$\Gamma \approx N_{22,100}\, \epsilon_{\rm prog}\, \epsilon_{\rm p\text{-}space}\, \epsilon_{\rm 3BH}\, \epsilon_{\rm merge}, \quad (6)$$

where $N_{22,100} = 6 \times 10^4\,{\rm Gpc}^{-3}\,{\rm yr}^{-1}$ is the number of stars formed with masses between 22 and 100 solar masses.

The quantity $\epsilon_{\rm prog}$ in Equation (6) is the ratio of BH triple progenitors to total BH progenitors. As in Silsbee & Tremaine (2017), we assume the following: 19% of systems with at least one BH progenitor are single systems, 56% are binaries, and 25% are triples. These percentages are consistent with Sana et al. (2014) who found these fractions of multiplicity for the O-stars in their sample. Given our mass distributions, for models A2, B2, and C2, we find a fraction $\epsilon_{\rm prog} = 0.04$ of triple progenitors with $(m_1, m_2, m_3) > 22\ M_\odot$, and for models A1, B1, and C1 we find a fraction $\epsilon_{\rm prog} = 0.06$ of triple progenitors in which the inner binary components have ZAMS mass $(m_1, m_2) > 22\ M_\odot$.

The quantity $\epsilon_{\rm p-space}$ is the fraction of parameter space that we are simulating relative to the full parameter space for massive triples that is covered by observations. This fraction is $\epsilon_{\rm p-space} \approx 0.35$ in our models and takes into account the fact that we are only simulating systems with $a_1(1-e_1^2) \gtrsim 11$ au initially. In order to estimate $\epsilon_{\rm p-space}$, we have assumed a maximum separation for the outer orbit of 6000 au because this is approximately the distance within which the companions to the massive stars in the sample of Sana et al. (2014) are resolved or spectroscopically identified.

Finally, $\epsilon_{\rm merge}$ is the fraction of dynamically stable BH triples formed in our models, which produce a BH merger. Roughly speaking, this fraction, ≈1%, is independent of the assumed distribution of natal kick velocities. This latter result can appear quite surprising: the change in linear momentum

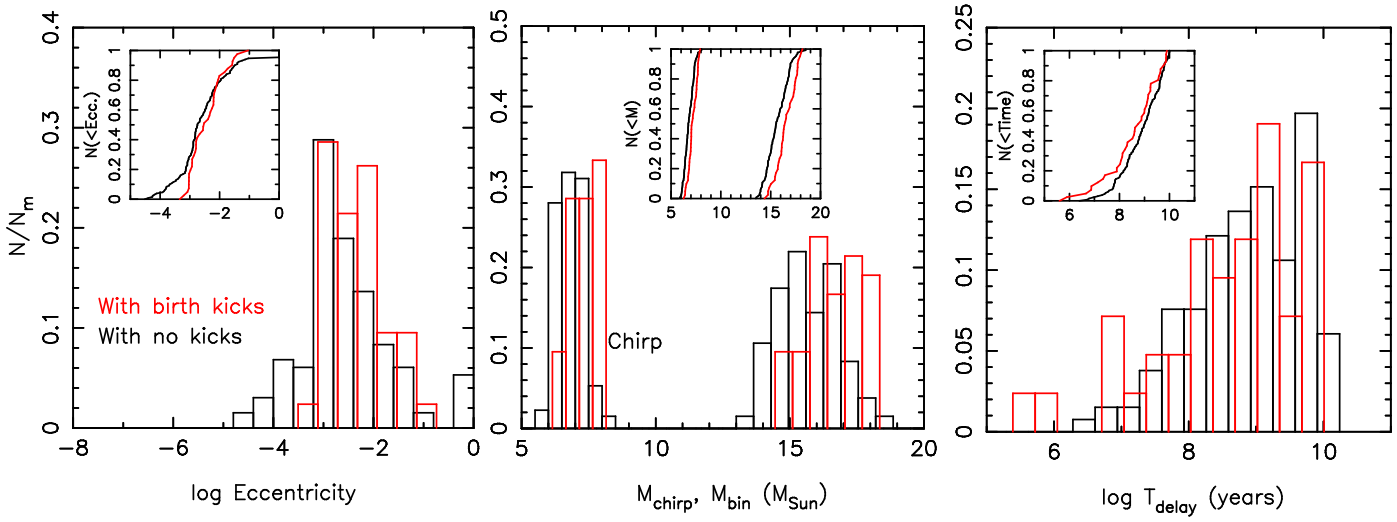

Figure 4. Properties of merging BH binaries. Distributions are normalized by the total number of mergers. The left panel gives the distribution of eccentricities at the moment the binaries first enter the aLIGO frequency band. The middle panel shows the distribution of total mass, and chirp mass of the merging BHs. The right panel gives their time delay distribution, i.e., the time from formation to coalescence. Red histograms and curves are for models B1, B2, C1, and C2 combined; black is for models A1 and A2.

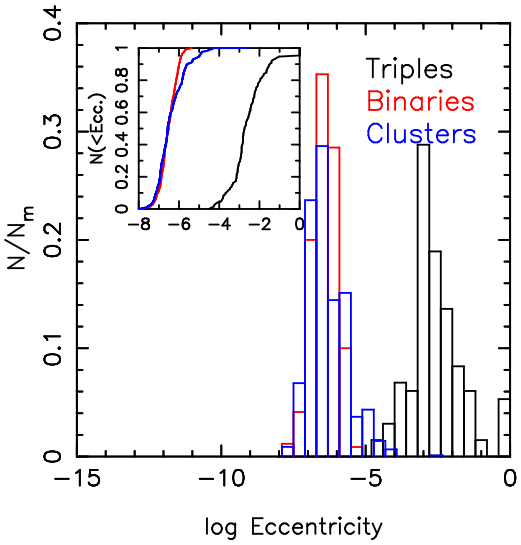

Figure 5. Distribution of eccentricities at the moment the BH binaries enter the aLIGO frequency band (10 Hz) for mergers produced by dynamical interactions in dense star clusters, massive binary stars, and massive triples (models A1+A2). Binaries formed in triples have much larger eccentricities than those formed through other channels.

instantaneously imparted to the exploding stars alters the orientation of orbital planes subsequent to BH formation and could result in a larger number of BH triples that are formed with initially high inclination. Consequently, one would expect a larger fraction of merging binaries in the non-zero-kick models (e.g., Silsbee & Tremaine 2017). Contrary to this expectation, our simulations suggest that this effect has a small impact on the resulting BH binary merger rate. We also note that $\epsilon_{\rm merge}$ appears to be approximately unaffected by the choice we make for the upper limit on the separation of the outer orbit.

Table 1 gives the results of our calculations. We estimate the BH merger rate in isolated triple systems in the field to be at most $\approx 1\,{\rm Gpc}^{-3}\,{\rm yr}^{-1}$.

Some of our models can be directly compared to the results of Silsbee & Tremaine (2017). For example, similar to our models A1 and A2, the latter authors also consider models where the BHs receive no natal kicks (see their Table 2). Their zero-kick models produce a merger rate of $\approx 6\,{\rm Gpc}^{-3}\,{\rm yr}^{-1}$, which is about six times larger than the merger rate inferred from our simulations. One reason for the discrepancy in the rate estimates is that Silsbee & Tremaine (2017) assume zero Blaauw kick (Blaauw 1961), which increases the chance that a triple in their zero-kick models will survive the formation of a BH, leading to higher merger rates. Moreover, Silsbee & Tremaine (2017) assume that BH triples are formed with initially random inclinations. However, in many of the highly inclined triples in our models, the two inner objects merge early during their main-sequence evolution. We also note that Silsbee & Tremaine (2017) used a somewhat different model for the period and mass distributions, and a shorter maximum simulation time. These differences with our models will also affect the merger rates, but not as significantly as the effects due to the more realistic inclination and kick distributions used in our simulations.

Silsbee & Tremaine (2017) also consider models with a non-zero natal kick velocity. In one of their models, they adopt a Gaussian kick velocity distribution with $\sigma \approx 40\,{\rm km\,s}^{-1}$, which results in a merger rate of $\approx 0.14\,{\rm Gpc}^{-3}\,{\rm yr}^{-1}$ (see their Table 2). This appears to be a few times smaller than the rate inferred from our models B1, B2 and C1, C2. We believe that the main reason for our higher merger rates in this case is that we implemented a zero kick for the very massive stars (Fryer & Kalogera 2001), which increases the number of systems that remain bound after BH formation.

5. Additional Considerations

5.1. Consequences of Non-secular Dynamics

As shown above in Figure 3, the merging binaries in our models evolve through a non-secular dynamical phase where the standard secular perturbation theory is expected to break down. This has important consequences on both the properties and the merger rate of binaries formed through the triple channel. These binaries will in fact have higher eccentricities because they enter the aLIGO band and a higher chance of

merging than what we would predict based on the standard secular equations of motion (Antonini & Perets 2012; Katz & Dong 2012; Antognini et al. 2014; Antonini et al. 2014, 2016).

To demonstrate the importance of the non-secular regime for the evolution of our binaries, we integrated all BH triples formed in our models using the orbit-averaged equations of motion (Blaes et al. 2002) up to a final integration time of 10 Gyr. In total, we find 79 mergers, which is a factor of 2.2 smaller than the total of 177 mergers we previously found. Moreover, the secular integrations did not produce any merging binaries with eccentricities larger than ≈0.1 at 10 Hz, while about 3% of all merging binaries that we evolved using the direct integrator had eccentricities larger than $(1-e_1)\lesssim 10^{-6}$ at 10 Hz (see Figures 4 and 5).

5.2. Effects Due to Flyby Encounters

In our simulations, many potential progenitors for BH mergers experience a collision already during the main-sequence evolution. As shown in Figure 2, this reduces the number of BH triple systems with inclination $I\approx 90^\circ$ which can later lead to a merger. However, the BH triple orbits may change significantly due to interactions with passing stars or with the local tidal field. If such changes are sufficiently violent to alter the inclination after the two BHs have formed, the fraction of triples that avoid a phase of mass transfer throughout the stellar evolution and can merge after the three stars have become BHs will be larger than the fraction given in Table 1.

Here, we briefly discuss the effect that encounters can have on the outer orbit of the BH triple, neglecting Galactic tides, which are typically less important for the systems we consider. Generally, the effect of encounters is largest on the outer orbit of the triple. The triple BH systems, which lead to mergers in our simulations, typically have $a_2\sim 10^4$ au, with outliers at roughly 10^3 and 10^5 au. We assume the encounters are impulsive, i.e., they give a velocity kick to the outer binary. The kick Δv to the orbital speed can be estimated as (e.g., Kaib & Raymond 2014, Equation (7))

$$\Delta v\sim \frac{3Ga_2 m_\star}{b_\star^2 v_\star}, \tag{7}$$

where $m_\star$, $v_\star$, and $b_\star$ are the mass, speed (at infinity), and closest approach distance of the perturbing star, respectively. The specific orbital angular momentum vector of the outer orbit is $\boldsymbol{j}=\boldsymbol{r}\times\boldsymbol{v}$, where $\boldsymbol{r}$ and $\boldsymbol{v}$ are the outer orbit relative orbital separation and velocity, respectively. The impulsive kick leads to an orbital velocity of $\boldsymbol{v}'=\boldsymbol{v}+\Delta\boldsymbol{v}$, whereas the position vector is assumed to be unchanged, i.e., $\boldsymbol{r}'=\boldsymbol{r}$. Assuming that the changes in $\hat{\boldsymbol{j}}$, i.e., the direction of the outer orbital angular momentum, are small, we expand the expression $\hat{\boldsymbol{j}}'=[\boldsymbol{r}\times(\boldsymbol{v}+\Delta\boldsymbol{v})]/||\boldsymbol{r}\times(\boldsymbol{v}+\Delta\boldsymbol{v})||$. Neglecting terms of the order of $(\Delta v)^3$ and higher, we obtain for the change of the inclination

$$\cos(\Delta i)=\hat{\boldsymbol{j}}\cdot\hat{\boldsymbol{j}}'\approx 1-\frac{1}{2}\frac{(\boldsymbol{r}\times\Delta\boldsymbol{v})^2}{j^2}-\frac{[\hat{\boldsymbol{j}}\cdot(\boldsymbol{r}\times\Delta\boldsymbol{v})]^2}{j^2}. \tag{8}$$

Averaging the above expression over all orientations of $\Delta\boldsymbol{v}$, assuming random directions of the passing stars and keeping $\boldsymbol{r}$ and $\hat{\boldsymbol{j}}$ fixed, this gives

$$\langle\cos(\Delta i)\rangle\approx 1-\frac{2}{3}\frac{r^2\Delta v^2}{j^2}\sim 1-\frac{6Gm_\star a_2^3(1+e_2)^2}{b_\star^4 v_\star^2}\frac{m_\star}{M}, \tag{9}$$

where $M=m_1+m_2+m_3$, e_2 is the outer orbital eccentricity, and we assumed that the outer binary is at apoapsis, where the effect of the encounter is strongest.

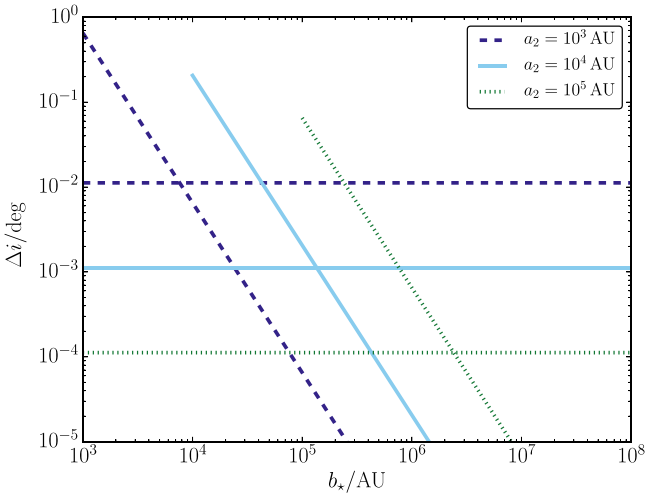

Figure 6. Typical change in the inclination of the outer orbit of a typical progenitor BH triple due to a flyby with closest approach distance $b_\star$ (see Equation (9)). Three different values of the outer semimajor axis are assumed: 10^3, 10^4, and 10^5 au. The horizontal lines show Δi averaged over $b_\star$. Refer to Section 5.2 for details.

In Figure 6, we show the inclination change Δi according to the simple estimate Equation (9) as a function of $b_\star$. We take three values of a_2, and set $m_1=m_2=m_3=7\,M_\odot$ and $e_2=0.6$, typical for the merging systems at the moment of BH formation. The perturber parameters are set to $m_\star=0.4\,M_\odot$ (a typical field star mass) and $v_\star=40\,\mathrm{km\,s^{-1}}$ (the typical velocity dispersion in the solar neighborhood). The lower and upper limits on $b_\star$ are set to $b_{\star,\min}=a_2$ and $b_{\star,\max}=2\pi v_\star\sqrt{a_2^3/(GM)}$, respectively. The upper limit corresponds to the value of $b_\star$ for which the perturber passage timescale, $\sim b_\star/v_\star$, is equal to the outer binary orbital period. If $b_\star$ is larger than $b_{\star,\max}$, we expect the changes to be secular (rather than impulsive); the latter are very small in low-density environments such as the field. The horizontal lines in Figure 6 show Δi averaged over $b_\star$, assuming $dN/db_\star\propto b_\star$.

From Figure 6, it is clear that individual encounters can only give rise to very small inclination changes, typically $\sim 10^{-3}$ degrees (for $a_2=10^4$ au), and no larger than $\sim 1^\circ$ (if $a_2=10^5$ au and the encounter is deeply penetrating the outer binary). However, the cumulative change of the inclination depends on the system age, in particular, the time before the merger, which can be as long as 10^{10} years. These potentially important effects will be considered in more detail in future work.

In order to demonstrate how stellar encounters could impact our merger rate estimates, we consider a new set of simulations, where we take the BH triple initial conditions from model A2 but now sampling the initial value of I randomly in $-1<\cos I<1$. The fraction of stable BH triples that lead to a merging BH binary in this new model are $\epsilon_{\rm merge}=0.015$. This corresponds to a merger rate of $\Gamma\approx 2.5\,\mathrm{Gpc^{-3}\,yr^{-1}}$.

5.3. BH Mergers from $a_1 \lesssim 10$ au

In the models of Table 1, we have set a minimum orbital separation to avoid mass transfer based on the maximum radius of a low-mass BH progenitor. However, stars more massive than 50 $M_\odot$ suffer from severe wind mass losses, such that they do not reach core helium burning before the Wolf–Rayet phase (i.e., losing their hydrogen envelopes). As a result, their maximum radii during their evolution is about an order of magnitude smaller as those for lower-mass BH progenitors. This means that there is a part of parameter space in which a triple BH could form that we did not consider.

In order to address the contribution of BH binaries that form from massive stars with $a_1(1-e_1^2) \lesssim 2500\,R_\odot$, we evolved an additional 25k systems in which we take $a_{2,\max} = 5\times10^6\,R_\odot$, $m_{3,\min} = 0.1\ M_\odot$, assuming no-kicks as in model A1 but now setting $250 \lesssim a_1(1-e_1^2) \lesssim 2500\,R_\odot$ and $(m_1, m_2) > 50\,M_\odot$. For this set of parameters $\epsilon_{\text{p-space}} \approx 0.3$, similar to our standard models. These simulations resulted in $\epsilon_{3\text{BH}} = 0.11$ and $\epsilon_{\text{merge}} = 0.01$, giving roughly the same fraction of merging binaries (i.e., $\epsilon_{3\text{BH}}\,\epsilon_{\text{merge}}$) as model A1. However, the fraction of all triples with $(m_1, m_2) > 50M_\odot$ is about 10 times less than triples with $(m_1, m_2) > 22\ M_\odot$, suggesting a total merger rate of $\Gamma \lesssim 0.1\,\text{Gpc}^{-3}\,\text{yr}^{-1}$ and a contribution at the 10% level in our models.

6. Conclusions

A large fraction (≈25%) of massive stars are observed to be in triple systems (Sana et al. 2014). In this paper, we have studied how the evolution of massive triples can lead to the formation of BH triple systems and how their subsequent dynamical evolution can result in the merger of two BHs. We study this problem using a combination of high-precision direct integrations (Mikkola & Merritt 2008) and a code that combines secular three-body dynamics with stellar evolution and their mutual influences (Toonen et al. 2016). Our approach allows us to make reliable predictions about the properties of the newly formed BH triples, and about the rates and properties of the merging binaries. The main conclusions of our study are summarized below.

(1) In our models with no natal kicks, about 20% of the massive triple stars evolve into a hierarchical BH triple system; in models that include non-zero natal kicks, this percentage is smaller, ≈5%, as many triples are disrupted during BH formation. About ≈1% of the BH triples that are formed in our models produce a merging BH binary. This latter fraction is roughly independent of the assumed distribution of natal kick velocities.

(2) The majority (132 out of 177) of BH mergers in our models are formed through a complex non-secular dynamical evolution, which cannot be adequately modeled using the standard (double-averaged) secular perturbation theory, even at the octupole level of approximation. Compared to direct three-body integrations, secular calculations underpredict the number of BH mergers by a factor ≈2 as well as the eccentricity of the merging binaries.

(3) We estimate the rate of BH mergers in isolated triples in the field to be in the range $(0.3\text{–}1.3)\,\text{Gpc}^{-3}\,\text{yr}^{-1}$. If the orbital inclinations of the BHs are efficiently randomized, for example, as a consequence of interactions with passing field stars, the resulting merger rate could be as large as $\approx 2.5\,\text{Gpc}^{-3}\,\text{yr}^{-1}$.

(4) Inspiraling BH binaries formed in field triples have significantly higher eccentricities than those formed through the evolution of field binaries or via dynamical interactions in dense star clusters. A few percent of merging binaries in our models enter the aLIGO frequency band with $(1-e_1) \lesssim 10^{-6}$. We conclude that measured eccentricities could provide a way to uniquely identify binary mergers formed through the evolution of massive triple stars.

F.A. acknowledges support from a CIERA postdoctoral fellowship at Northwestern University. S.T. acknowledges support from the NetherlandsResearch Council NWO (grant VENI [nr. 639.041.645]). A.S.H. acknowledges support from the Institute for Advanced Study, and NASA NNX14AM24G grant.

References

Abbott, B. P., Abbott, R., Abbott, T. D., et al. 2016a, PhRvL, 116, 061102
Abbott, B. P., Abbott, R., Abbott, T. D., et al. 2016b, ApJL, 818, L22
Abbott, B. P., Abbott, R., Abbott, T. D., et al. 2016c, PhRvL, 116, 241103
Abbott, B. P., Abbott, R., Abbott, T. D., et al. 2016d, ApJL, 833, L1
Amaro-Seoane, P., Audley, H., Babak, S., et al. 2017, arXiv:1702.00786
Antognini, J. M., Shappee, B. J., Thompson, T. A., & Amaro-Seoane, P. 2014, MNRAS, 439, 1079
Antonini, F., Chatterjee, S., Rodriguez, C. L., et al. 2016, ApJ, 816, 65
Antonini, F., Murray, N., & Mikkola, S. 2014, ApJ, 781, 45
Antonini, F., & Perets, H. B. 2012, ApJ, 757, 27
Antonini, F., & Rasio, F. A. 2016, ApJ, 831, 187
Arzoumanian, Z., Chernoff, D. F., & Cordes, J. M. 2002, ApJ, 568, 289
Banerjee, S. 2017, MNRAS, 467, 524
Belczynski, K., Dominik, M., Bulik, T., et al. 2010, ApJL, 715, L138
Belczynski, K., Repetto, S., Holz, D. E., et al. 2016, ApJ, 819, 108
Blaauw, A. 1961, BAN, 15, 265
Blaes, O., Lee, M. H., & Socrates, A. 2002, ApJ, 578, 775
Breivik, K., Rodriguez, C. L., Larson, S. L., Kalogera, V., & Rasio, F. A. 2016, ApJL, 830, L18
Chatterjee, S., Rodriguez, C. L., Kalogera, V., & Rasio, F. A. 2017, ApJL, 836, L26
Chen, X., & Amaro-Seoane, P. 2017, arXiv:1702.08479
Dosopoulou, F., & Kalogera, V. 2016a, ApJ, 825, 70
Dosopoulou, F., & Kalogera, V. 2016b, ApJ, 825, 71
Duchêne, G., & Kraus, A. 2013, ARA&A, 51, 269
Fabrycky, D., & Tremaine, S. 2007, ApJ, 669, 1298
Fryer, C. L., & Kalogera, V. 2001, ApJ, 554, 548
Hamers, A. S., Pols, O. R., Claeys, J. S. W., & Nelemans, G. 2013, MNRAS, 430, 2262
Haster, C.-J., Antonini, F., Kalogera, V., & Mandel, I. 2016, ApJ, 832, 192
Hobbs, G., Lorimer, D. R., Lyne, A. G., & Kramer, M. 2005, MNRAS, 360, 974
Holman, M., Touma, J., & Tremaine, S. 1997, Natur, 386, 254
Hurley, J. R., Pols, O. R., & Tout, C. A. 2000, MNRAS, 315, 543
Hut, P. 1981, A&A, 99, 126
Kaib, N. A., & Raymond, S. N. 2014, ApJ, 782, 60
Katz, B., & Dong, S. 2012, arXiv:1211.4584
Kimpson, T. O., Spera, M., Mapelli, M., & Ziosi, B. M. 2016, MNRAS, 463, 2443
Kobulnicky, H. A., Kiminki, D. C., Lundquist, M. J., et al. 2014, ApJS, 213, 34
Kozai, Y. 1962, AJ, 67, 591
Kroupa, P. 2002, Sci, 295, 82
Lidov, M. L. 1962, P&SS, 9, 719
Mandel, I., & de Mink, S. E. 2016, MNRAS, 458, 2634
Mardling, R. A., & Aarseth, S. J. 2001, MNRAS, 321, 398
Mikkola, S., & Merritt, D. 2008, AJ, 135, 2398
Naoz, S. 2016, ARA&A, 54, 441
Naoz, S., Farr, W. M., Lithwick, Y., Rasio, F. A., & Teyssandier, J. 2013, MNRAS, 431, 2155
Nishizawa, A., Sesana, A., Berti, E., & Klein, A. 2017, MNRAS, 465, 4375
Perets, H. B., & Kratter, K. M. 2012, ApJ, 760, 99

Peters, P. C. 1964, PhRv, 136, 1224
Rodriguez, C. L., Morscher, M., Pattabiraman, B., et al. 2015, PhRvL, 115, 051101
Sana, H., de Mink, S. E., de Koter, A., et al. 2012, Sci, 337, 444
Sana, H., Le Bouquin, J.-B., Lacour, S., et al. 2014, ApJS, 215, 15
Sepinsky, J. F., Willems, B., Kalogera, V., & Rasio, F. A. 2007, ApJ, 667, 1170
Silsbee, K., & Tremaine, S. 2017, ApJ, 836, 39
Thompson, T. A. 2011, ApJ, 741, 82
Toonen, S., Hamers, A., & Portegies Zwart, S. 2016, ComAC, 3, 6
Toonen, S., & Nelemans, G. 2013, A&A, 557, A87
Toonen, S., Nelemans, G., & Portegies Zwart, S. 2012, A&A, 546, A70
Wen, L. 2003, ApJ, 598, 419